Magnetic and crystal field properties of $DyRh_2Si_2$ and $ErRh_2Si_2$ from ^{161}Dy and ^{166}Er Mossbauer spectroscopy

1989 J. Phys.: Condens. Matter 1 9231

(http://iopscience.iop.org/0953-8984/1/46/015)

J. Phys.: Condens. Matter 1 (1989) 9231–9241. Printed in the UK

Magnetic and crystal field properties of $DyRh_2Si_2$ and $ErRh_2Si_2$ from ^{161}Dy and ^{166}Er Mössbauer spectroscopy

K Tomala†‡, J P Sanchez† and R Kmieć§

† Institut de Physique et Chimie des Matériaux (GMI) and Centre de Recherches Nucléaires, 67037 Strasbourg Cédex, France

§ Institute of Nuclear Physics, Cracow, Poland

Received 21 April 1989

Abstract. Detailed ^{161}Dy and ^{166}Er Mössbauer measurements on $DyRh_2Si_2$ and $ErRh_2Si_2$ are reported. The 4f contribution to H_{hf} and e^2qQ was calculated by self-consistently diagonalising the exchange and the crystal-field Hamiltonian. This approach allowed us to reproduce the temperature dependence of the hyperfine parameters as well as enabling the canting of the Dy moments at low temperatures. The crystal field level scheme deduced was used to explain the relaxation spectra observed in the ordered state of $ErRh_2Si_2$. The saturation Dy (9.7 μ_B) and Er (8.64 μ_B) moments were found to be close to the respective free ion values. The best agreement with the experimental data was obtained with $H_{mol}(0) = 167.5$ kOe, $B_2^0 = -1.17$ K, $B_4^0 = 3.2 \times 10^{-3}$ K for $DyRh_2Si_2$ and $H_{mol}(0) = 43$ kOe, $B_2^0 = 0.45$ K, $B_4^0 = -1.3 \times 10^{-3}$ K, $|B_4^4| = 3.6 \times 10^{-3}$ K for $ErRh_2Si_2$.

1. Introduction

The ternary rare earth silicides RT_2Si_2 (R = rare earth, T = 3d, 4d or 5d transition metal) were shown to exhibit very exciting physical properties ranging from superconductivity to heavy fermion behaviour (Rogl 1984, Parthé and Chabot 1984, Ott and Fisk 1987). Most of them crystallise in the body-centred tetragonal structure of the $ThCr_2Si_2$-type (space group I4/mmm). These inter-metallics usually order magnetically at low temperatures and present different types of magnetic structure with magnetic moments generally localised only at the R-site (Szytuła and Leciejewicz 1989).

The present study reports on detailed ^{161}Dy and ^{166}Er Mössbauer measurements of the temperature dependence of the hyperfine field (H_{hf}) and of the quadrupole coupling constant (e^2qQ) at the R-site in R Rh_2Si_2 (R = Dy, Er). Both hyperfine interaction parameters are sensitive to the nature of the electronic state of the R^{3+} ions, as fashioned by the magnetic interactions and the crystalline electric field (CEF) produced by the neighbouring ions in the lattice. The hyperfine interaction data, when supplemented by bulk magnetisation and neutron diffraction results, are expected to provide information about the strength of the molecular field (H_{mol}) and the crystal field parameters (B_n^m).

$DyRh_2Si_2$ has already been extensively studied by bulk magnetisation (Felner and Nowik 1983, 1984) and neutron diffraction (Melamud *et al* 1984) and some preliminary

‡ On leave from Institute of Physics, Jagellonian University, Cracow, Poland.

0953-8984/89/469231 + 11 $02.50

^{161}Dy Mössbauer results were reported (Felner and Nowik 1983, 1984, Sanchez *et al* 1988). $DyRh_2Si_2$ was shown to order antiferromagnetically at 55 K with Dy moments along the *c* axis and to exhibit a second transition around 15 K. The latter was initially ascribed to the onset of itinerant magnetism with very small magnetic moment at the Rh site. This explanation was, however, ruled out by the neutron data, which demonstrated that the transition at 15 ± 3 K is due to a reorientation of the Dy moments from the c-axis. The canting angle θ at 4.2 K was found to amount to 19 ± 5° and the Dy moment (9.9 ± 1 μ_B) to be close to its free-ion value.

Magnetisation and neutron diffraction data of $ErRh_2Si_2$ were reported by Szytuła *et al* (1984). They showed that $ErRh_2Si_2$ is a collinear antiferromagnetic ($T_N \simeq 13$ K) with Er moments (7.74 ± 0.27 μ_B at 4.2 K) in the basal plane. Some preliminary ^{166}Er Mössbauer results were presented at ICM 88 (Sanchez *et al* 1988).

The paper has been organised in the following way. In § 2 we give a brief account of the experimental details and describe the experimental results. In § 3 we discuss our results in the frame of an exchange and crystal-field Hamiltonian and present our conclusions concerning the molecular-field and crystal-field parameters acting at the R-site.

2. Experimental procedure and results

2.1. Experimental procedure

$DyRh_2Si_2$ and $ErRh_2Si_2$ were prepared by arc melting, under a purified argon atmosphere, of stoichiometric amounts of the constituents. Melting was repeated several times in order to ensure homogeneity. Then the samples were vacuum annealed in silica tubes for one week at 900 °C and slowly cooled down. The samples analysed by x-ray diffraction did not reveal any impurity phase. Lattice constants evaluated from least-squares fit of the x-ray line positions were found to be in good agreement with earlier published values (Felner and Nowik 1983, 1984).

^{161}Dy Mössbauer spectroscopy measurements were performed using a sinusoidal drive motion of a neutron-irradiated $^{160}Gd_{0.5}{}^{162}Dy_{0.5}F_3$ source kept at room temperature. The velocity scale was calibrated using metallic Dy (H_{hf} = 5689(3) kOe, e^2qQ = 124.9(2) mm s^{-1}, Bertheir *et al* (1975)). Because of the large photoabsorption cross section for the 25.6 keV gamma rays by the Rh atoms, absorber thickness was carefully optimised (about 33 mg cm^{-2} of $DyRh_2Si_2$). Even then, a one week measurement for each spectrum was necessary to obtain good quality data. The gamma rays were detected using a high resolution Si(Li) detector.

^{166}Er Mössbauer spectra were obtained using a neutron-activated $Y_{0.6}Ho_{0.4}H_2$ source kept at about 10 K in order to reduce relaxation linebroadening. The 80.6 keV gamma rays were counted with a Ge(Li) diode. An absorber containing 330 mg cm^{-2} of $ErRh_2Si_2$ was used. The velocity calibration of the spectrometer was performed using a ^{57}Co/Rh source and a metallic iron absorber.

The RRh_2Si_2 absorbers were maintained in liquid helium (or nitrogen) cryostats that enable measurements to be made at different temperatures with an accuracy of ±0.1 K. The static effective magnetic-field spectra were directly least-squares fitted to the hyperfine parameters by constraining the relative absorption energies and intensities of the Lorenztian lines to the theoretical values. Some erbium spectra were analysed using a relaxation model that will be described in § 3.3.

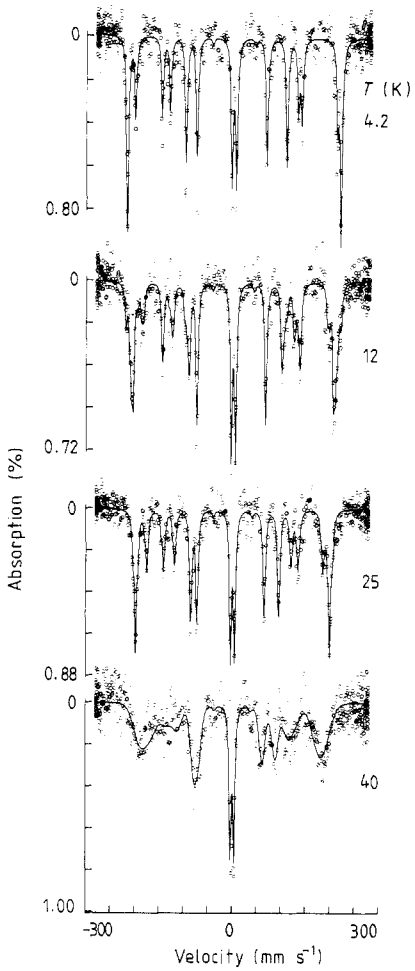

Figure 1. ^{161}Dy Mössbauer spectra of $DyRh_2Si_2$ at different temperatures. The spectrum taken at 4.2 K was fitted with a single component. The spectra recorded at 12, 25 and 40 K were analysed taking into account the distribution of the hyperfine parameters (see text).

2.2. *Experimental results*

2.2.1. $DyRh_2Si_2$. Figure 1 shows spectra taken at temperatures between 4.2 and 40 K. The 4.2 K spectrum is well analysed with a single set of hyperfine parameters with the electric-field gradient axis parallel to the hyperfine field, i.e. to the magnetisation (table 1). Notice that the linewidth is, however, slightly broader than the one found in metallic Dy ($W = 4.4$ mm s^{-1}). All the other spectra recorded in the magnetically ordered state (i.e. at $T < 55$ K) present severe linebroadenings, which were attributed to distributed hyperfine parameters. The possible influence of relaxation processes is ruled out from the lineshape of the two inner lines, which remain sharp and well separated (Wickman 1966, Wickman and Wertheim 1968). The 12 K data can be fitted either with four independent magnetic (plus quadrupole) sub-spectra or with a histogram of hyperfine fields with linearly correlated quadrupolar interaction, the standard deviation of the latter parameter being $\sigma_Q \simeq 11$ mm s^{-1}. The spectra at 25 and 40 K are best fitted with either a histogram method or a Gaussian distribution of H_{hf} and a unique value for the quadrupolar interaction (table 1). It was found that both the average hyperfine field and its standard deviation are not sensitive to the method we used to analyse the spectra.

Table 1. Hyperfine interaction parameters for ^{161}Dy in $DyRh_2Si_2$ (see text).

T (K)	H_{hf}(kOe)	σ_H[b] (kOe)	e^2qQ[a] (mm s^{-1})	δ_{IS}[c] (mm s^{-1})	W[a] (mm s^{-1})
4.2	5513 (20)	—	105.7 (1.0)	1.0 (1)	5.0(2)
12	5305 (30)	160 (20)	89.2 (1.5)	0.9 (1)	5.0[d]
25	5033 (30)	73 (10)	71.6 (1.5)	0.9 (1)	5.0[d]
40	4719 (50)	340 (30)	61.1 (2.5)	0.9 (1)	5.0[d]

[a] For E = 25.6 keV in ^{161}Dy: 1 mm s^{-1} = 8.5576×10^{-8} eV = 20.69 MHz.
[b] σ_H: standard deviation of the hyperfine-magnetic-field distribution.
[c] Isomer shift relative to the source.
[d] Linewidth W constrained in the least-squares fit procedure.

Above the Néel temperature, the resonance spectra practically collapse to a broad single line whose width at 300 K, amounting to about 14 mm s^{-1}, is essentially due to the unresolved quadrupolar interaction.

The origin of the hyperfine parameter distributions has not yet been well established. The occurrence of a complicated magnetic structure is ruled out from the neutron diffraction data, which showed that $DyRh_2Si_2$ is a collinear antiferromagnet (Melamud *et al* 1984). Therefore we attributed the linebroadenings observed to a possible interchange of the Rh and Si atoms in the $ThCr_2Si_2$-type structure. This is expected to induce small changes in the molecular- and crystal-field parameters and thus in the hyperfine data. The following arguments may support our assumption. First, it was reported that R $RhSi_3$ phases that derive from the $ThCr_2Si_2$ structure exist for light rare earth elements (Wang *et al* 1985). Secondly, table 1 shows that the distribution of H_{hf} is wider at 12 K than at 25 K. At 12 K, in the canted-structure phase, the ground-state wavefunction is quite sensitive to small fluctuations of the CEF parameters. On the other hand, at 25 K, i.e. when the magnetisation is parallel to the c axis, the nature of the ground state is mainly determined by the axial B_2^0 CEF term and the molecular field; but when B_2^0 is negative (as here, see below), the ground-state wavefunction is rather unsensitive to the relative magnitude of the exchange- and crystal-field interactions: thus, the hyperfine parameters are expected to be less distributed. Finally, it should be pointed out that the interchange of the Rh and Si atoms cannot be detected by our x-ray analysis.

2.2.2. $ErRh_2Si_2$. Figure 2 shows some representative spectra taken at temperatures between 1.5 and 18 K. The temperature dependence of the spectra clearly evidences three types of behaviour. Between 1.5 and 6 K, the data are well represented by a single site static hyperfine interaction Hamiltonian with collinear hyperfine-field- and electric-field-gradient axes (table 2). Between 8 and 12 K, the resonance shape is modified by relaxation effects. At 8 K, where the spectral shape is not yet strongly distorted by relaxation effects, it is still possible to analyse the data with a static effective-field Hamiltonian, when allowing different linewidths for the $\Delta m = 0, \pm 1$ and ± 2 transitions. Notice that this procedure gives reliable average values for H_{hf} only. Thus at 8 K and at higher temperatures, i.e. 10 and 12 K, it was necessary to fit the data with a relaxation model that takes into account the nature and occupation of the electronic levels, as determined from the molecular and crystal fields acting at the Er site (see below). Collapse of the magnetic hyperfine structure was found to occur at about 14 K, in good agreement with the already quoted Néel temperature obtained from bulk magnetisation measurements (Szytuła *et al* 1984). Above 15 K, one observes a single broadened

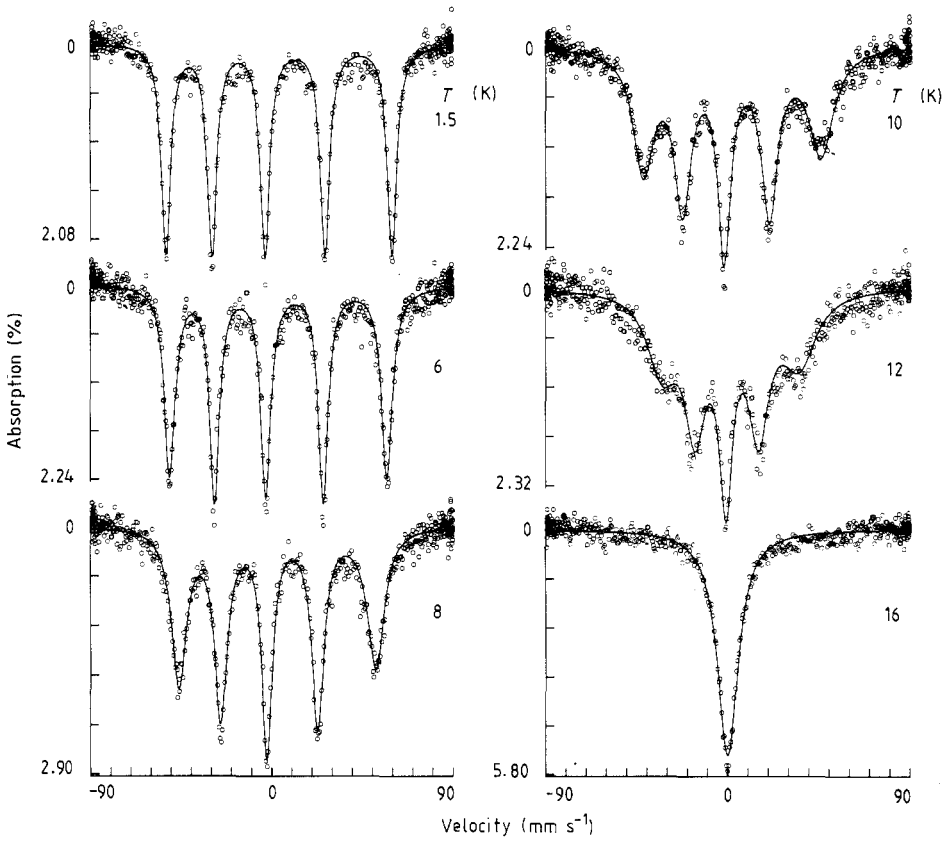

Figure 2. ^{166}Er Mössbauer spectra of $ErRh_2Si_2$ at different temperatures. The spectrum taken at 1.5 K and 6 K were fitted using a static Hamiltonian, while the data obtained at higher temperatures were least-squares analysed, using a relaxation model (see text).

Table 2. Hyperfine interaction parameters for ^{166}Er in $ErRh_2Si_2$ (see text).

T (K)	H_{hf} (kOe)	e^2qQ^a (mm s^{-1})	W^a (mm s^{-1})	$\Omega^{a,b}$ (GHz)
1.5	7357 (20)	13.8 (3)	5.6 (2)	—
4.2	7307 (20)	13.7 (3)	5.4 (2)	—
6	7073 (20)	12.5 (3)	5.8 (2)	—
8	6401 (20)	—	6.8 (2)	—
	6453[c]	10.7[c]	6.4 (2)	50 (7)
10	5475[c]	8.2[c]	7.5 (2)	36 (5)
12	3827[c]	5.4[c]	7.8 (3)	42 (6)

[a] For $E = 80.6$ keV in ^{166}Er: 1 mm s^{-1} = 26.8709 × 10^{-8} eV = 64.973 MHz.
[b] The relaxation rate is defined as $\Omega = \hbar/\tau$ where τ is the relaxation time.
[c] Values obtained as a thermodynamical average from a level scheme used to fit the relaxation spectra (see text).

resonance line whose width ($W \simeq 12.4$ mm s^{-1})—constant up to at least 18 K—is due to residual relaxation effects and to the unresolved quadrupolar interaction.

3. Discussion

3.1. Hamiltonian and hyperfine interaction parameters

The temperature dependence of the hyperfine parameters, the canting of the Dy moments and the relaxation effects observed in the Er compounds were explained using an exchange-crystal-field Hamiltonian. The crystal-field interaction for tetragonal symmetry was truncated to second- and fourth-order CEF B_n^m coefficients (for simplicity, B_6^0 and B_6^4 were set to zero) and we adopted the two-dimensional molecular-field approximation where the R moments are confined to the xz plane. The z and x-axis were chosen parallel and perpendicular to the c axis. Then, the Hamiltonian that describes the electronic behaviour of the Dy^{3+} and Er^{3+} ions has the following form (Bak 1974, Takano *et al* 1987a, b):

$$\mathcal{H} = B_2^0\hat{O}_2^0 + B_4^0\hat{O}_4^0 + B_4^4\hat{O}_4^4 - \lambda N(g_J\mu_B)^2\{\hat{J}_x\langle J_x\rangle + \hat{J}_z\langle J_z\rangle\} \tag{1}$$

where B_n^m are the crystal-field parameters and $\hat{O}_n^m$ the Stevens operator equivalents tabulated, for example, by Hutchings (1964). λ is the molecular field constant, N the Avogadro number and g_J the Landé factor. $\hat{J}_x$ and $\hat{J}_z$ are the angular moment operators and $\langle J_x\rangle$ and $\langle J_z\rangle$ their thermal average. It is convenient to relate λ, in the absence of crystal field, to the Néel temperature T_N^0 and to the molecular field H_{mol} using the following expressions:

$$T_N^0 = \lambda N(g_J\mu_B)^2 J(J+1)/3k_B \qquad g_J\mu_B H_{mol} = 3k_B T_N^0/(J+1) \tag{2}$$

where J is the total angular momentum and k_B the Boltzmann constant.

Some initial guessed values for the molecular and B_2^0 CEF parameters can be obtained from the bulk magnetisation and ^{155}Gd Mössbauer measurements in $GdRh_2Si_2$ (Felner and Nowik 1983, Buschow and de Mooij 1986, Czjzek *et al* 1989). T_N^0 values of 47.7 and 17.2 K for $DyRh_2Si_2$ and $ErRh_2Si_2$, respectively, can be estimated from the Néel temperature of $GdRh_2Si_2$ ($T_N = 106(1)$ K) Czjzek *et al* (1989) using the De Gennes scaling: $T_N^0 \propto (g_J - 1)^2 J(J+1)$. The B_2^0 coefficients can be computed from the ^{155}Gd quadrupolar data ($e^2qQ = -3.35(2)$ mm s^{-1}), which directly provide the lattice electric-field gradient (eq^{lat}), which is related to B_2^0 by

$$B_2^0 = -\alpha_J eq^{lat}\langle r^2\rangle(1-\sigma_2)/4(1-\gamma_\infty). \tag{3}$$

With selected values of the shielding factors, $(1-\gamma_\infty) = 60$, $(1-\sigma_2) = 0.4$ and tabulated $\langle r^2\rangle$ (Freeman and Desclaux 1979) and α_J Stevens factors (Hutchings 1964), one obtains $B_2^0 = -1.93$ K for $DyRh_2Si_2$ and $B_2^0 = 0.70$ K for $ErRh_2Si_2$. At this stage it is worth pointing out that the sign of B_2^0 gives indications for the easy direction of magnetisation, i.e. parallel to the c axis when B_2^0 is positive and in the basal plane when B_2^0 is negative.

The hyperfine-field and the quadrupolar interactions are commonly described as a sum of several contributions:

$$H_{hf} = H_{hf}^{4f} + H_{hf}^{core} + H_{hf}^{ce} \tag{4a}$$

$$e^2\tilde{q}Q = e\tilde{q}^{4f}Q + e\tilde{q}^{lat}Q \tag{4b}$$

where H_{hf}^{4f} and $e^2\tilde{q}^{4f}Q$ represent the contributions of the localised 4f electrons. H_{hf}^{core} is

the core polarisation field and H_{hf}^{ce} the conduction-electron contribution. eq^{lat} is the EFG produced by the lattice charges. The possible contribution of the conduction electrons is included in eq^{lat}.

The 4f contribution to H_{hf} and eqQ were calculated from the eigenvalues and eigenvectors obtained by self-consistently diagonalising the Hamiltonian in (1). With $|\Gamma^k\rangle$ the wavefunction of the kth electronic level and E^k its energy, the following equations were used to calculate the components of the hyperfine field $(H_{hf}^{4f})_i$ and quadrupolar interaction tensor $(eq^{4f}Q)_{ij}$ $(i, j = x, y, z)$

$$(H_{hf}^{4f})_i = H_{hf}^{4f}(\text{free ion}) \sum \langle\Gamma^k|\hat{J}_i|\Gamma^k\rangle \exp(-E^k/k_B T) \Big/ J \sum_k \exp(-E^k/k_B T) \tag{5a}$$

$$(eq^{4f}Q)_{ij} = eq^{4f}Q\,(\text{free ion}) \sum_k \langle\Gamma^k|\tfrac{3}{2}(\hat{J}_i\hat{J}_j + \hat{J}_j\hat{J}_i) - \delta_{ij}\hat{J}^2|\Gamma^k\rangle/[3J^2 - J(J+1)]$$

$$\times \exp(-E^k/k_B T) \Big/ \sum_k \exp(-E^k/k_B T). \tag{5b}$$

The free ion values for Dy^{3+} were taken as discussed in a previous paper (Tomala *et al* 1989) to be H_{hf}^{4f}(free ion) = 5930(30) kOe and $e^2q^{4f}Q$ (free ion) = 135(1) mm s^{-1}. For Er^{3+} the following free-ion estimates were generally accepted (Bleaney 1972): H_{hf}^{4f}(free ion) = 7800(80) kOe and $e^2q^{4f}Q$(free ion) = 16.3(7) mm s^{-1}.

The 4f contribution to H_{hf} for $DyRh_2Si_2$ was calculated as $H_{hf}^{4f} = [(H_{hf}^{4f})_x^2 + (H_{hf}^{4f})_z^2]^{1/2}$ and its direction relative to the c axis was obtained from $\tan\theta = \langle J_x\rangle/\langle J_z\rangle$ where $\langle J_x\rangle$ and $\langle J_z\rangle$ are thermal averages of the suitable matrix elements. The component $(eq_{z'z'} = V_{z'z'})$ of the quadrupole-interaction tensor in the magnetic-field direction was computed using the general formula (Amoretti *et al* 1987):

$$V_{z'z'} = \tfrac{1}{2}V_{zz}[3\cos^2(\theta) - 1 + \eta\sin^2\theta\cos(2\varphi)] + V_{xz}\sin(2\theta)\cos\varphi$$
$$+ V_{xy}\sin^2\theta\sin(2\varphi) + V_{yz}\sin(2\theta)\sin\varphi \tag{6}$$

where η is the asymmetry parameter and θ, φ the polar angles which define the direction of H_{hf}^{4f} (i.e. the magnetisation) in the CEF reference frame (x, y, z); $\varphi = 0$ in our specific case since the moments are confined in the (xz) plane.

For $ErRh_2Si_2$ Hamiltonian (1) takes a simplified form: the molecular field is restricted to its x-component (the moments are in the basal plane); H_{hf}^{4f} is then equal to $(H_{hf}^{4f})_x$ and (6) shows that $V_{z'z'} = -\frac{1}{2}V_{zz}$.

The other contributions to H_{hf} and to e^2qQ in (4*a*, *b*) were estimated from the ^{155}Gd Mössbauer data in $GdRh_2Si_2$. For an S-state ion, the 4f contributions vanish. The field of −312(1) kOe (Czjzek *et al* 1989) measured in $GdRh_2Si_2$ provides a direct evaluation of $(H_{hf}^{core} + H_{hf}^{ce})$ in R Rh_2Si_2 when scaling the Gd data with the spin $S = (g_J - 1)J$ of the R element (−223(1) and −134(1) kOe for Dy and Er, respectively). The lattice component $e^2q_{z'z'}^{lat}Q$ along the hyperfine-field direction were computed from $e^2q_{zz}^{lat}Q$ (^{155}Gd), applying (6) with $\eta^{lat} = 0$ (tetragonal symmetry) and using the quadrupole-moment values of $Q_g(^{155}Gd) = 1.30(2)b$ (Tanaka *et al* 1982), $Q_g(^{161}Dy) = 2.35(16)b$ and $Q_{ex}(^{166}Er) = -1.59(15)b$ (Stevens 1981). It follows that $e^2q_{z'z'}^{lat}Q(^{166}Er) = -2.2(0.5)$ mm s^{-1} and $e^2q_{z'z'}^{lat}Q(^{161}Dy) = -10.2\,(3\cos^2(\theta) - 1)$ mm s^{-1}.

The temperature dependences of the 4f contributions were calculated by self-consistently diagonalising the Hamiltonian (1) at each temperature. The temperature variation of $(H_{hf}^{core} + H_{hf}^{ce})$ was taken to be proportional to $\langle J\rangle/J$. It should be mentioned

that, for $DyRh_2Si_2$, $e^2q^{lat}_{z'z'}Q$ varies with temperature unless the Dy moments are along the c axis.

The Néel temperatures may be calculated by following the temperature dependence of the magnetisation or by using the following relation (Noakes and Shenoy 1982):

$$T_N = 2\mathcal{H}_{exch}(g_J - 1)^2\langle J_i^2(T_N)\rangle_{CEF} = T_N^0\langle J_i^2(T_N)\rangle_{CEF}/J(J+1) \qquad (7)$$

where $\langle J_i^2\rangle$ is the expectation value of $\hat{J}_i^2$ under the influence of the CEF alone in the Hamiltonian (1): $i = z$ for $DyRh_2Si_2$ and $i = x$ for $ErRh_2Si_2$. Both methods give similar T_N values. A first estimate of T_N can be obtained from T_N^0 and B_2^0 scaled from $GdRh_2Si_2$. But it turned out that the calculated T_N (96.5 and 23.5 K for Dy and Er, respectively) are too high compared to the experimental values. Thus both T_N^0 and B_2^0 so estimated should be decreased to allow agreement with experimental data.

In the following two sections we will describe and discuss in more detail the method we used to extract the CEF and molecular-field parameters from our experimental data on $DyRh_2Si_2$ and $ErRh_2Si_2$.

3.2. Crystal electric field and molecular field parameters in $DyRh_2Si_2$

Before going further in the discussion it should be recalled that B_2^0 is negative and that the occurrence of a canting of the Dy moments requires positive B_4^0. As previously emphasised (Tomala *et al* 1989) the hyperfine parameters are not sensitive to the actual value of B_4^4 when B_2^0 is negative and large.

Agreement between calculated and experimental results was achieved as follows.

Step 1. T_N^0 was decreased step by step from its De Gennes scaled value and couples of T_N^0, B_2^0 were chosen to reproduce the experimental T_N approximately using (7).
Step 2. For each pair of T_N^0 and B_2^0, the Hamiltonian (1) was selfconsistently diagonalised, with B_4^0 taken to fit the experimental data at 4.2 K.
Step 3. With a proper set of T_N^0, B_2^0 and B_4^0 we calculated the temperature dependence of H_{hf} and e^2qQ and computed T_N as well as the thermal variation of the canting angle θ.

It was found that only narrow ranges of T_N^0 (41.5 to 43.5 K), B_2^0(−1.15 to −1.20 K) and B_4^0(0.00315 to 0.00325 K) values were able to reproduce satisfactorily the whole experimental data. Calculated $H_{hf}(T)$ and $e^2qQ(T)$ curves, shown in figure 3, were obtained with the following parameters: $T_N^0 = 42.5$ K (or $H_{mol}(0) = 167.5$ kOe); $B_2^0 = -1.17$ K and $B_4^0 = 0.00325$ K. The saturation Dy moment (9.7 μ_B) is found to be close to the free ion value of 10 μ_B. The canting angles calculated ($\theta = 24.9°$ at 4.2 K) and the reorientation temperature ($T_R = 14.5(5)$ K) given in the inset to figure 3 are in reasonable agreement with experimental results. On the other hand, the theoretical $T_N = 67(2)$ K is slightly higher than the experimental value of 55 K. This misfit may arise from anisotropic exchange interactions (Ishida *et al* 1986) not taken into account in the Hamiltonian (1).

3.3. Crystal electric field, molecular field and relaxation in $ErRh_2Si_2$

Some conclusions concerning the signs of the B_n^m coefficients can already be drawn from the $GdRh_2Si_2$ and $DyRh_2Si_2$ data: B_2^0 should be positive and B_4^0 must be taken as negative (the β_J Stevens factors for Dy and Er have opposite signs). Since we assumed that the magnetisation in the easy plane is along the x axis, B_4^4 has to be negative. It should be

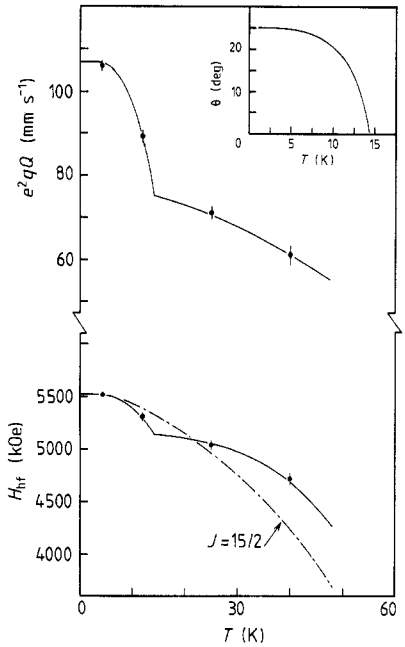

Figure 3. Temperature dependence of the hyperfine-field and quadrupole interaction in $DyRh_2Si_2$. The full curves correspond to the results of calculations described in the text. The Brillouin curve for free-ion behaviour (chained curve) was shown for comparison. The temperature dependence of the Dy magnetic moment canting angle θ is given in the inset.

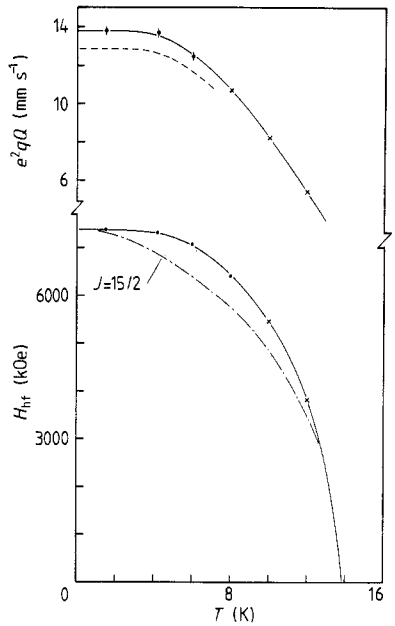

Figure 4. Temperature dependence of the hyperfine field and quadrupole interaction in $ErRh_2Si_2$. The full curves correspond to the calculations described in the text. The Brillouin curve for free-ion behaviour (chained curve) was shown for comparison. For e^2qQ, the broken curve represents the results obtained when taking the free-ion value and lattice contribution given in the text; the full curve was obtained by shifting the calculated curve to fit with the 1.5 K data. The crosses represent average values of the hyperfine parameters, as calculated from the electronic-level scheme used to least-squares fit the relaxation spectra shown in figure 2.

noticed that positive B_4^4 only means that the magnetisation lies along the (110)-axis. Thus at this stage only the absolute value of B_4^4 can be determined.

The method we used to describe the experimental results is given below.

Step 1. As for $DyRh_2Si_2$, T_N^0 was changed step by step from De Gennes value and B_2^0 was chosen to give T_N in the range 13 to 15 K.

Step 2. For each pair of T_N^0, B_2^0, we selected B_4^0 and B_4^4 parameters that fit the data at 1.5 K.

Step 3. With the proper choice of T_N^0 and B_n^m parameters, we calculated the temperature dependence of H_{hf} (up to 8 K) and of e^2qQ (up to 6 K).

At this point one should remark that it was impossible to reproduce simultaneously H_{hf} and e^2qQ values at 1.5 K. This is either due to the improper choice of the free ion parameters (they are known with rather large uncertainties) or to the procedure used to estimate the lattice contribution to e^2qQ (the possible influence of slightly different lattice parameters is not taken into account). Nevertheless, the shape of the temperature

dependence of the hyperfine parameters is not influenced by the choice of the free-ion values or the scaling from the gadolinium results.

Step 4. The relaxation spectra at 8, 10 and 12 K were analysed as follows. The Hamiltonian (1) was diagonalised for each set of suitable T_N^0, B_n^m coefficients and the electronic-level scheme was determined. The relaxation spectra were least-squares fitted using the Wickman formalism for ferromagnetic relaxation (Wickman 1966, Wickman and Wertheim 1968) and constraining the energies and hyperfine-interaction parameters of the electronic levels. All levels with Boltzmann occupation higher than 1% were taken into account (i.e. five levels). Furthermore it was assumed that relaxation can take place only between adjacent levels weighted by their Boltzmann factors. In a first attempt the data were fitted with the linewidth W fixed to its 1.5 K value and only the baseline, total amplitude and relaxation rate Ω as free parameters. It turned out that the quality of the fit can be improved when allowing a small increase of the linewidth, especially for spectra taken at 10 and 12 K (figure 2).

As for $DyRh_2Si_2$ only narrow ranges of T_N^0 (9.75 to 9.95 K), B_2^0(0.40 to 0.50 K), B_4^0(−0.0010 to −0.0015 K) and $|B_4^4|$(0.0027 to 0.0043 K) values were shown to give a reasonable account of the experimental data. The calculated and experimental values of H_{hf} and e^2qQ are presented in figure 4. The saturated Er moment (8.64 μ_B) is slightly below the free ion- value of 9 μ_B. The theoretical curves were obtained with the following set of parameters: $T_N^0 = 9.85$ K (i.e. $H_{mol}(0) = 43$ kOe), $B_2^0 = 0.45$ K, $B_4^0 = -0.0013$ K and $|B_4^4| = 0.0036$ K. The same set of parameters was taken to reproduce the relaxation spectra shown in figure 2. The average hyperfine-interaction parameters obtained from the electronic-level scheme used to fit the relaxation spectra are listed in table 2 and represented by crosses in figure 4. The theoretical Néel temperature of 13.8 K agrees well with the experimental value of 13 K. Finally, the relaxation rate Ω was found to be nearly constant (table 2), as expected over such a narrow range of temperatures.

4. Summary and conclusions

The present work reports the results of a ^{161}Dy and ^{166}Er Mössbauer study of $DyRh_2Si_2$ and $ErRh_2Si_2$. The occurrence of distributed hyperfine-interaction parameters in the ordered state of $DyRh_2Si_2$ suggests some mixing between the Rh and Si atoms that occupy the 4d and 4e sites respectively, in the $ThCr_2Si_2$ structure. The analysis of the saturation hyperfine-field and quadrupole-interaction data shows that the Dy (9.7 μ_B) and Er (8.64 μ_B) moments are close to their respective free ion values. The temperature dependences of H_{hf} and e^2qQ were explained straightforwardly in the framework of an exchange- and crystal-field Hamiltonian. This approach enabled us to estimate the molecular field as well as the second- and fourth-order crystal-field parameters acting at the R-atoms in the $R Rh_2Si_2$ compounds. The relaxation behaviour observed in the ordered state of $ErRh_2Si_2$ was reproduced satisfactorily using a relaxation model that takes into account all occupied crystal-field levels. It was furthermore shown that the exchange-crystal-field Hamiltonian with the same set of parameters used to explain the hyperfine data gives a reliable description of the canting of the Dy moments observed at low temperatures.

Acknowledgments

We gratefully acknowledge the technical contributions of A Bonnenfant and R Poinsot. One of the authors (KT) is grateful to the Centre de Recherches Nucléaires (IN_2P_3) Strasbourg for its hospitality and financial support. This work was partially supported by CPBP 01.12 in Poland.

References

Amoretti G, Bogé M, Fournier J M, Blaise A and Wojakowski A 1987 *J. Magn. Magn. Mater.* **66** 236–52
Bak P 1974 *J. Phys. C: Solid State Phys.* **7** 4097–103
Berthier Y, Barak J and Barbara B 1975 *Solid State Commun.* **17** 153–5
Bleaney B 1972 *Magnetic Properties of Rare Earth Metals* ed. R J Eliott (London and New York: Plenum) p 383
Buschow K H J and de Mooij D B 1986 *Philips J. Res.* **41** 55
Czjzek G, Oestreich V, Schmidt H, Łatka K and Tomala K 1989 *J. Magn. Magn. Mater.* **79** 42–56
Felner I and Nowik I 1983 *Solid State Commun.* **47** 831–4
—— 1984 *J. Phys. Chem. Solids* **45** 419–26
Freeman A J and Desclaux J P 1979 *J. Magn. Magn. Mater.* **12** 11–21
Hutchings M T 1964 *Solid State Physics* ed. F Seitz and D Turnbull (New York and London: Academic) vol 16 p 227
Ishida S, Asano S and Ishida J 1986 *J. Phys. Soc. Japan* **55** 936–45
Melamud M, Pinto H, Felner I and Shaked H 1984 *J. Appl. Phys.* **55** 2034–5
Noakes D R and G K Shenoy 1982 *Phys. Lett.* **91A** 35–6
Ott H R and Fisk Z 1987 *Handbook on the Physics and Chemistry of the Actinides* vol 5 ed. A J Freeman and G H Lander (Amsterdam: North Holland) p 85
Parthé E and Chabot B 1984 *Handbook of the Physics and Chemistry of the Rare Earths* vol 6 ed K A Gschneidner Jr and L Eyring (Amsterdam: North Holland) p 113
Rogl P 1984 *Handbook on the Physics and Chemistry of the Rare Earths* Vol 6 ed. K A Gschneider Jr and L Eyring (Amsterdam: North Holland) p 335
Sanchez J P, Tomala K and Kmieć R 1988 *J. Physique Coll.* **49** C8-435–6
Stevens J G 1981 *Handbook of Spectroscopy* vol 3 ed. J W Robinson (Boca Raton: CRC) p 403
Szytuła A and Leciejewicz J 1989 *Handbook on the Physics and Chemistry of Rare Earths* vol 12 ed. K A Gschneidner Jr and L Eyring (Amsterdam: Elsevier) p 133
Szytuła A, Ślaski M, Ptasiewicz-Bak H, Leciejewicz J and Zygmunt A 1984 *Solid State Commun.* **52** 395–8
Takano Y, Ohhata K and Sekizawa K 1987a *J. Magn. Magn. Mater.* **70** 242–4
—— 1987b *J. Magn. Magn. Mater.* **66** 187–93
Tanaka Y, Lanbacher D B, Steffen R M, Shera E B, Wohlfart H D and Hoehn M V 1982 *Phys. Lett.* **108B** 8–10
Tomala K, Sanchez J P and Kmieć R 1989 *J. Phys.: Condens. Matter* **1** 4415–23
Wang Xian-Zhong, Lloret B, Wee Lam Ng, Chevalier B, Etourneau J and Hagenmuller P 1985 *Rev. Chimie Minérale* **22** 711–21
Wickman H H 1966 *Mössbauer Effect Methodology* vol 2 ed. I J Gruverman (New York: Plenum) p 39
Wickman H H and Wertheim G K 1968 *Chemical Applications of the Mössbauer Spectroscopy* ed. V I Goldanskii and R H Herber (New York: Academic) p 317